Carbon–Oxygen Bond Cleavage Reactions by Electron Transfer. 1. Electrochemical Studies on the Formation and Subsequent Reaction Pathways of Cyanoanisole Radical Anions

Miles D. Koppang, Neil F. Woolsey, and Duane E. Bartak*

Contribution from the Department of Chemistry, University of North Dakota, Grand Forks, North Dakota 58202. *Received September 12, 1983*

Abstract: The radical anions of three isomers of cyanoanisole have been electrochemically generated and subsequently shown to react by at least three different reaction pathways in dry *N,N*-dimethylformamide (DMF). The *o*-cyanoanisole radical anion (E_{pc} = −2.3 V vs. SCE) dimerizes ($k_2 = 3.2 \times 10^2$ M^{-1} s^{-1}) to form an intermediate dimeric dianion. The dianion, which can be oxidized (E_{pa} = −1.1 V vs. SCE), undergoes a slow intramolecular disproportionation reaction to form *o*-cyanophenoxide ion, methide ion, and unreduced substrate ($k_3 = 1.9 \times 10^{-2}$ s^{-1}). Subsequent protonation results in the formation of methane and *p*-cyanophenol in an overall two-electron process. The *m*-cyanoanisole radical anion (E_{pc} = −2.3 V vs. SCE) is very stable ($t_{1/2} > 10^3$ s) under anhydrous DMF conditions. Overall, slow carbon–carbon bond cleavage with loss of cyanide occurs competitively with β carbon–oxygen bond cleavage to produce anisole and *m*-cyanophenol, respectively. The final products of the reduction of *p*-cyanoanisole are *p*-cyanophenol and methane; however, the radical anion of *p*-cyanoanisole (E_{pc} = −2.5 V vs. SCE) undergoes a relatively rapid unimolecular fragmentation reaction ($k_1 = 7$ s^{-1}). The initial products of the fragmentation are *p*-cyanophenoxide ion and the methyl radical, which is reduced further to methide ion. Hydrogen atom abstraction reactions by the methyl radical can also occur in the bulk solution to produce methane.

Although there are extensive reports on carbon–halogen bond cleavage by both electrochemical and chemical means,[1-3] there are limited data on reductive carbon–oxygen bond cleavage in ethers. This is probably due to the inertness of the carbon–oxygen bond in an ether vs. the carbon–halogen bond in organic halides. The initial product of electron transfer, a radical anion, often cleaves to produce an organic radical and an anion in these types of cleavage reactions. Both the strength of the carbon–heteroatom bond and the leaving-group ability of the resultant anion play important roles in determining the reactivity of these radical anions. Literature reports indicate that it is sometimes necessary to insert an activating group on the organic moiety to make the reduction potential of ethers more positive; however, this in turn stabilizes the resulting radical anion so as to preclude rapid unimolecular fragmentation.

The reductive cleavage of carbon–oxygen bonds in alcohols,[4] pinacols,[5] phenols,[6] esters,[7-13] and ethers[14,15] by electrochemical means has been reported by several workers. Simonet studied the electroreduction of a series of alkyl ethers including benzylic, allylic, vinylic, and allenic ethers in both protic and aprotic solvents.[14] Carbon–oxygen bond cleavage for benzylic and allylic ethers was reported to proceed by a two-electron mechanism to the alcohol and hydrocarbon.

$$ROR + 2e^- \xrightarrow{2H^+} ROH + RH$$

More recently, Hawley has examined the mechanism for reductive bond cleavage of 9-hydroxy- and 9-methoxyfluorenes.[15] Heterolytic carbon–oxygen bond cleavage resulted in the formation of a fluorenyl radical and OR^- (R = H, CH_3); however, the overall chemistry was dominated by the acidity of the fluorenyl (C_9) proton.

The above studies were concerned with the cleavage of ethers in which only aliphatic-type carbons were bonded to oxygen. Studies on the elctrochemical cleavage of alkyl aryl ether bonds in which one of the carbon atoms bonded to oxygen is of the aryl type are sparse. Le Guyader has reported on the electrochemical reduction of *p*-nitroanisole in sulfuric acid/ethanol mixtures in which carbon–oxygen bond cleavage as well as nitro-group reduction occurs to produce *p*-aminophenol.[16] Tallec observed similar formation of 2-amino-4-nitrophenol upon reduction of 2,4-dinitroanisole in acidic media.[17] Cleavage studies using chemical reductants have also been reported with an emphasis on product analysis and not mechanistic details. For example, Eisch used lithium/biphenyl to cleave anisole with a 55% yield of phenol.[18] Angelo studied the cleavage of several ethers including benzyl phenyl ether, which yielded 48% phenol upon treatment with sodium/naphthalene.[19] Itoh and co-workers have shown that regioselective cleavage of aryl decyl ethers can be accomplished by variation in the metal reductant and the presence of an organic electron-transfer mediator.[20]

Rieger et al. reported on the electrochemistry of *p*-cyanoanisole as a part of a comprehensive study on the ESR and electrochemistry of substituted benzonitrile radical anions.[21] Although

(1) For a recent review on organic halide reductions, see: Hawley, M. D., in "Encyclopedia of Electrochemistry of the Elements"; Bard, A. J., Lund, H., Eds.; Marcel Dekker: New York, Vol. XIV, 1980; Chapters 1–5.
(2) Holy [Holy, N. L. *Chem. Rev.* **1974**, *74*, 243] reviews homogeneous electron-transfer reactions of aromatic halides and ethers.
(3) Rifi [Rifi, M. R. In "Techniques of Electroorganic Synthesis"; Weinberg, N. L., Ed.; Wiley: New York, 1975; Part II] reviews organic halides on pp 170–191, carbon–oxygen cleavage on p 249, and [Rifi, M. R. In "Organic Electrochemistry"; Baizer, M. M., Ed.; Marcel Dekker: New York, 1973; pp 279–314] reviews organic halide reductions. Lund [Lund, H. p. of 767 of preceding reference] reviews carbon–oxygen bond cleavage.
(4) Lund, H.; Doupeux, H.; Michel, M. A.; Mousset, G.; Simonet, J. *Electrochim. Acta* **1974**, *19*, 629.
(5) Michel, M. A.; Mousset, G.; Simonet, J.; Lund, H. *Electrochim. Acta* **1975**, *20*, 143.
(6) Shono, T.; Matsumura, Y.; Tsubata, K.; Sugihara, Y. *J. Org. Chem.* **1979**, *44*, 4508.
(7) Martigny, R.; Michel, M. A.; Simonet, J. *J. Electroanal. Chem.* **1976**, *73*, 373.
(8) Lund, H. *Acta Chem. Scand.*, **1960**, *14*, 1927.
(9) Given, P. H.; Peover, M. E.; *Nature (London)* **1959**, *184*, 1064.
(10) Berenjian, N.; Utley, J. H. P.; *J. Chem. Soc., Chem. Commun.* **1979**, 550.
(11) Coleman, J. P.; Naser-ud-din; Gilde, H. G.; Utley, J. H. P.; Weedon, B. C. L.; Eberson, L. *J. Chem. Soc., Perkin Trans. 2* **1973**, 1903.
(12) Coleman, J. P.; Gilde, H. G.; Utley, J. H. P. Weedon, B. C. L. *J. Chem. Soc. D* **1970**, 738.
(13) Mairanovsky, V. G. *Angew. Chem., Int. Ed. Engl.* **1976**, *15*, 281 and references therein.
(14) Santiago, E.; Simonet, J. *Electrochim. Acta* **1975**, *20*, 853.
(15) Nuntnarumit, C.; Hawley, M. D. *J. Electroanal. Chem.* **1982**, *133*, 57.
(16) Le Guyader, M. *Bull. Soc. Chim. Fr.* **1966**, 1858.
(17) Tallec, A. *Ann. Chim. (Paris)* **1968**, *3*, 347.
(18) Eisch, J. J. *J. Org. Chem.* **1963**, *28*, 707.
(19) Angelo, B. *Bull. Soc. Chim. Fr.* **1966**, 1091.
(20) Itoh, M.; Yoshida, S.; Ando, T.; Miyaura, N.; *Chem. Lett.* **1976**, 271.

0002-7863/84/1506-2799$01.50/0

Table I. Coulometric Data for the Reduction of the Cyanoanisoles[a]

entry	compound	concn, mM	E(applied),[b] V	n	products[c]
1	o-cyanoanisole	16	-2.4	1.0	46% o-cyanophenol, 47% o-cyanoanisole, methane
2	o-cyanoanisole	16	-2.4	2.0	94% o-cyanophenol, 6% o-cyanoanisole, methane
3	m-cyanoanisole	16	-2.4	1.7	63% m-cyanoanisole, 6% m-cyanophenol, 12% anisole
4	m-cyanoanisole	41	-2.4	1.0	81% m-cyanoanisole, 6% m-cyanophenol, 4% anisole
5	p-cyanoanisole	32	-2.6	2.0	74% p-cyanophenol, 19% p-cyanoanisole, methane
6	p-cyanoanisole	50	-2.6	2.0	90% p-cyanophenol, 5% p-cyanoanisole, methane
7	p-cyanoanisole	100	-2.6	0.8	39% p-cyanophenol, 62% p-cyanoanisole

[a] All electrolyses were conducted in 0.2 M TBAP-DMF. [b] Potentials are in volts vs. aqueous saturated calomel electrode. [c] The yields of all products except methane were determined by high-pressure liquid chromatography and are calculated on the basis of the original amount of cyanoanisole. Methane identification was accomplished by gas chromatography of head gas in the electrochemical cell.

p-cyanoanisole was reduced (E_p = -2.95 V vs. Ag-$AgClO_4$) at a dropping mercury electrode, no ESR signal was observed in an ESR flow system. The absence of the radical anion in the microwave cavity apparently indicated decomposition of the radical anion in the time domain necessary for transfer of the sample from the electrochemical cell to the microwave cavity. We report herein the reductive cleavage reaction pathways for p-cyanoanisole (an alkyl aryl ether) and two related isomers, o- and m-cyanoanisole.

Results and Discussion

o-Cyanoanisole. 1. Cyclic Voltammetry. The reductive electrochemical behavior of o-cyanoanisole (**1**) is illustrated in Figure 1. The cyclic voltammograms show one reduction wave at -2.32 V, which is electrochemically quasi-reversible. Upon reversal of the voltage scan at -2.6 V, a reoxidation wave is noted at -2.26 V. The ratio of peak currents (i_{pa}/i_{pc}) for this couple at a concentration of 0.62 mM increases with increasing scan rate and approaches unity at 0.1 V s^{-1}. The peak current ratio decreases with increasing concentration (Figure 1b), indicating disappearance of the radical anion by a process other than unimolecular fragmentation. A new oxidation wave is noted at -1.1 V; the height of this wave increases concomitantly with the decrease of the oxidation wave at -2.26 V. Successive cycles with a cathodic switching potential of -2.6 V and an anodic switching potential of -0.8 V result in a relative increase in the height of the oxidation wave at -1.1 V. Furthermore, cycling through the oxidation wave at -1.1 V results in a relative increase in the reduction wave at -2.32 V on the second cathodic scan when compared to the use of an anodic hold at this potential for the time necessary to scan to and from the former anodic switching potential of -0.8 V (e.g., if scan rate is 0.3 V s^{-1}, hold for 6 s before scanning back in the negative direction). Thus, at lease one of the products of the irreversible oxidation at -1.1 V is o-cyanoanisole.

2. Controlled Potential Electrolysis. A series of electrolysis experiments was carried out under controlled potential conditions at -2.4 V vs. SCE (Table I). If the electrolysis is stopped after the addition of 1 F mol^{-1}, analysis of the resultant solution shows that approximately 50% of the ether has been cleaved to o-cyanophenoxide ion and methane (Table I). Complete electrolysis of the solution after the addition of 2F mol^{-1} results in approximately 90% formation of the o-cyanophenol via an apparent β-cleavage reaction with respect to the aryl moiety. No benzonitrile (α-cleavage) or anisole (cyanide cleavage) was detected by gas chromatography or HPLC. In addition, methylated forms of o-cyanophenol, which could result from methyl radical attack on the phenoxide, were not observed by either gas chromatographic or HPLC analysis of the electrolysis solutions.

3. Kinetics for Disappearance of the Radical Anion and Formation of Products. Since the cyclic voltammetric data indicated that the lifetime of the radical anion of **1** is a function of concentration, single and double potential step chronoamperometric experiments were carried out to determine the reaction order kinetics for reduced **1**. Single potential step chronoamperometric experiments at an applied potential of -2.6 V vs. SCE produced

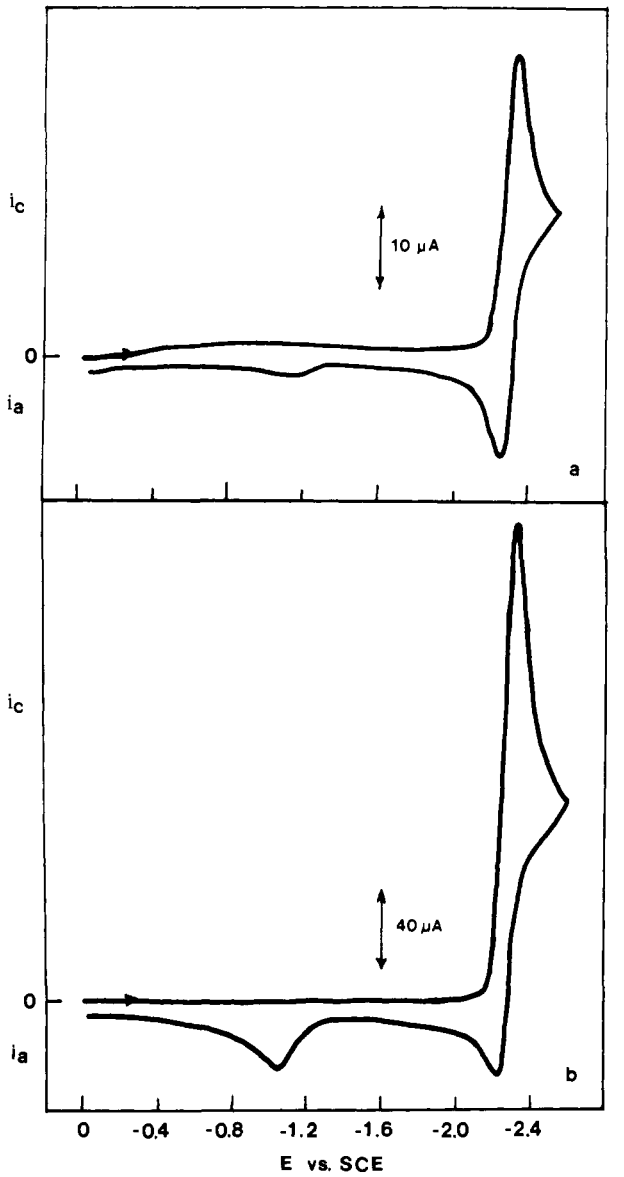

Figure 1. Cyclic voltammograms in 0.2 M TBAP-DMF at a scan rate of 0.1 V s^{-1}: (a) 6.2 × 10^{-4} M o-cyanoanisole, (b) 4.6 × 10^{-3} M o-cyanoanisole. The planar platinum electrode area is ~0.25 cm^2.

a constant $it^{1/2}/C$ value of 37 A $s^{1/2}$ mol^{-1} cm^3 (10 ms < t < 3 s) (geometrical area of electrode, 0.25 cm^2). This value can be compared to a value of 37 A $s^{1/2}$ mol^{-1} cm^3, which was obtained from a similar experiment on m-tolunitrile, which is reduced via a one-electron, diffusion-controlled process. At times greater than 3 s, the $it^{1/2}/C$ value for **1** increased with increasing time indicating kinetic control of the overall electrode reaction.

Double potential step chronoamperometry was accomplished with a potential step to -2.6 V to produce the radical anion of

(21) Rieger, P. H.; Bernal, I.; Reinmuth, W. H.; Fraenkel, G. K. J. Am. Chem. Soc. 1963, 85, 683.

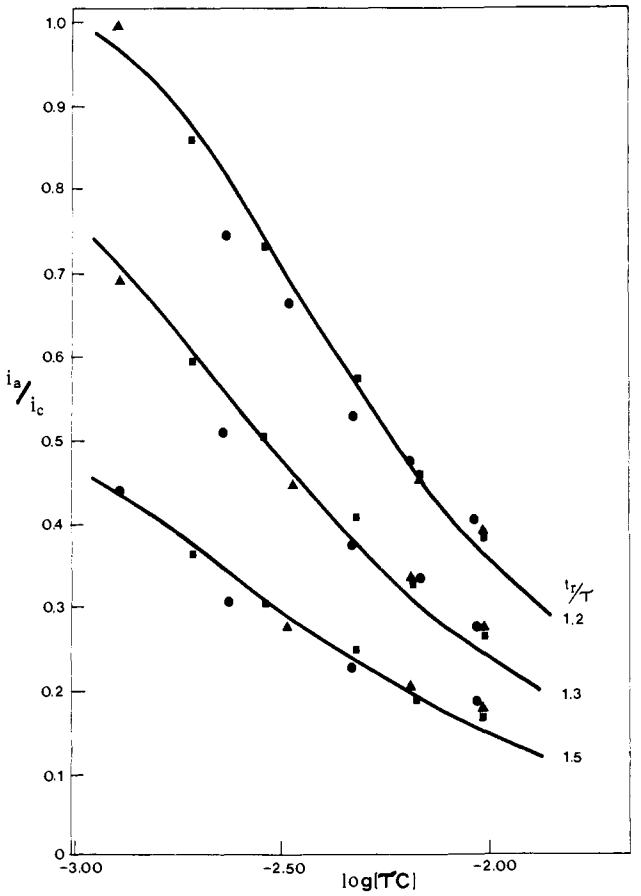

Figure 2. Double potential step chronoamperometric data for the disappearance of the *o*-cyanoanisole radical anion in 0.2 M TBAP–DMF. The solid curves were obtained by computer simulation[22] of the processes described by eq 1 and 2 with $k_2 = 3.2 \times 10^2$ M^{-1} s^{-1} for the following ratios of t_r/τ: (A) 1.2, (B) 1.3, and (C) 1.5. The cathodic electrolysis time is designated by τ; the total electrolysis time (anodic and cathodic) is symbolized by t_r. The points are the experimental data with *o*-cyanoanisole concentrations: (●) 4.63×10^{-3} M; (▲) 6.48×10^{-3} M; (■) 9.72×10^{-3} M.

1 during the time window for the diffusion-controlled process (10 ms $< t <$ 3 s) at the electrode surface. Upon generation of the radical anion for a period of time (τ), the potential was stepped back to the initial potential of −2.0 V in order to reoxidize the remaining radical anions of **1**. The ratio of anodic current to cathodic current (i_a/i_c) was determined as a function of the radical anion generation time (τ) and the concentration of the ether. A summary of the results of the double potential step chronoamperometric data is presented in Figure 2. In addition to varying the cathodic generation time (τ) and concentration of **1**, the current ratio was obtained at three different ratios of total electrolysis time to cathodic electrolysis time (t_r/τ). These data were compared to a digital simulated working curve[22] for the reaction sequence in eq 1 and 2. Good agreement between the data and

$$\mathrm{ArOCH_3} + e^- \rightleftarrows \mathrm{ArOCH_3^{-}\cdot} \quad (1)$$

$$2\mathrm{ArOCH_3^{-}\cdot} \xrightarrow{k_2} \text{products} \quad (2)$$

Ar = *o*-cyanophenyl

the working curve suggests that the *o*-cyanoanisole radical anion disappears by an irreversible second-order process with a rate constant of 3.2×10^2 M^{-1} s^{-1}.

The exhaustive electrolysis data (vide ante) indicate that the overall electron stoichiometry of the electrode reaction is two, with carbon–oxygen bond cleavage to form *o*-cyanophenoxide. Single potential step chronoamperometry was used to measure the rate

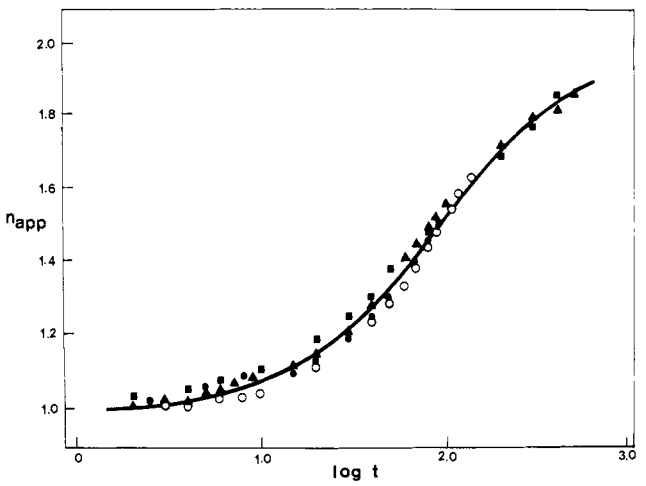

Figure 3. Single potential step chronoamperometric data for the change in electron stoichiometry for the reduction of *o*-cyanoanisole in 0.2 M TBAP–DMF. The solid curve was obtained by computer simulation[22,24] of eq 5 and 6 with a first-order rate constant of 1.9×10^{-2} s^{-1} (k_3). The experimental data are the points with the concentrations of *o*-cyanoanisole: (■) 3.2×10^{-4} M; (▲) 6.4×10^{-4} M; (○) 2.4×10^{-3} M; (●) 6.5×10^{-3} M.

of change in electron stoichiometry from times at which the reaction was a one-electron diffusion-controlled process ($t <$ 3 s) to times at which the stoichiometry was two electrons/molecule with concurrent product formation. Figure 3 is a summary of the single step data for **1**, which is normalized with respect to the diffusion-controlled, one-electron reduction of *m*-tolunitrile so that $n_{app} = (it^{1/2}/C)/(it^{1/2}/C)_{m\text{-tolunitrile}}$. The value of n_{app} was determined as a function of time (1 s $< t <$ 800 s) and was found to be independent of concentration (0.32–6.5 mM). Since the data indicate that the formation of *o*-cyanophenoxide ion is significantly slower than the disappearance of the *o*-cyanoanisole radical anion, an intermediate species is necessary between the radical anion and products in the reaction channel. A possible intermediate, which is not further reducible at −2.6 V, is a dimeric dianion, $(\mathrm{ArOCH_3})_2^{2-}$, as in eq 2A and 3.

$$2\mathrm{ArOCH_3^{-}\cdot} \xrightarrow{k_2} (\mathrm{ArOCH_3})_2^{2-} \quad (2A)$$

$$(\mathrm{ArOCH_3})_2^{2-} \xrightarrow{k_3} \mathrm{ArO^-} + \mathrm{CH_3^-} + \mathrm{ArOCH_3} \quad (3)$$

$$\mathrm{CH_3^-} + \mathrm{SH} \rightarrow \mathrm{CH_4} + \mathrm{S^-} \quad (4)$$

The formation of a dimeric dianion intermediate, which resulted from radical anion dimerization and underwent slow intramolecular electron transfer, has been postulated in the reduction of *o*-fluorobenzonitrile.[23] However, in that case, the dimeric dianion decomposed by an aryl carbon–halogen bond cleavage to form the *o*-cyanophenyl anion and fluoride ion. In the *o*-cyanoanisole case, decomposition of the dianion apparently proceeds by a carbon–oxygen bond cleavage, which is β to the ring to form *o*-cyanophenoxide and methide ion.

Since the rate of disappearance of radical anion of **1** was much more rapid than the appearance of products, the above reaction sequence (eq 1–3) was computer simulated as eq 5 and 6. The

$$2\mathrm{ArOCH_3} + 2e^- \xrightarrow{\text{rapid}} (\mathrm{ArOCH_3})_2^{2-} \quad (5)$$

$$(\mathrm{ArOCH_3})_2^{2-} \xrightarrow[\text{slow}]{k_3} \mathrm{ArO^-} + \mathrm{CH_3^-} + \mathrm{ArOCH_3} \quad (6)$$

Ar = *o*-cyanophenyl

resultant working curve is the solid line in Figure 3; the data, which

(22) Feldberg, S. W. *Electroanal. Chem.*, **1969**, *3*, 199.

(23) Houser, K. J.; Bartak, D. E.; Hawley, M. D.; *J. Am. Chem. Soc.* **1973**, *95*, 6033.

(24) Evans et al. [Evans, D. H.; Rosanske, T. W.; Jimenez, P. J. *J. Electroanal. Chem.* **1974**, *51*, 449] report a closed form solution of the mechanism described by eq 5 and 6.

were obtained at four different concentrations (0.32–6.5 mM), are in excellent agreement with the theoretical curve with a rate constant (k_3) of 1.9×10^{-2} s^{-1} for the dianion decomposition reaction. This value can be compared to that obtained for the decomposition of a fluoro-substituted dianion ($k \approx 1.0 \times 10^{-2}$ s^{-1}), which resulted from the dimerization of *o*-fluorobenzonitrile.[23]

Since the kinetic data indicate the importance of a dimeric dianion intermediate, it appears reasonable that the irreversible oxidation wave observed at −1.1V is the initial oxidation of the dianion to a radical anion of the dimer. Upon formation of the radical anion, rapid carbon–carbon bond cleavage occurs because of the energy gained in the rearomatization back to **1**. The initial result is the formation of **1** and the radical anion of **1**. Further oxidation of the radical anion of **1** then results in an overall two-electron wave for this process with the formation of *o*-cyanoanisole. The cyclic voltammetric data are consistent with this hypothesis since cycling the potential through the oxidation wave at −1.1 V produces a relatively larger amount of **1** at the electrode surface for reduction on the second cathodic scan (vide ante).

***m*-Cyanoanisole. 1. Cyclic Voltammetry.** An electrochemically reversible couple ($i_{pa}/i_{pc} = 1$, $\Delta E_p = 60$ mV) is observed for *m*-cyanoanisole (**2**) with $E_{pc} = -2.30$ V and $E_{pa} = -2.24$ V vs. SCE at a scan rate of 0.02 V s^{-1}. The current function value ($i_{pc}/v^{1/2}C$) had a value of 188 ± 8 A $s^{1/2}$ $V^{-1/2}$ mol^{-1} cm^3 on a planar platinum electrode of area 0.25 cm^2. This value is consistent with the current function of *m*-tolunitrile (181 ± 4 A $s^{1/2}$ mol^{-1} cm^3), which is a one-electron, diffusion-controlled process.

2. Chronoamperometry. Single potential step chronoamperometric experiments were carried out by stepping from an initial potential of −2.00 V to a final potential of −2.50 V. The resultant $it^{1/2}/C$ value of 160 ± 5 A $s^{1/2}$ mol^{-1} cm^3, which was obtained on a shielded platinum electrode (geometric area of 0.95 cm^2), was constant from times of 10 ms–640 s. This value can be compared to 162 ± 8 A $s^{1/2}$ mol^{-1} cm^3 for *m*-tolunitrile over the same time window. Thus, the above data indicate that **2** is reduced to a relatively stable anion radical, which has a half-life of at least 10^3 s.

3. Controlled Potential Electrolysis. Electrolysis experiments were carried out at an applied potential of −2.40 V vs. SCE. Although there was an initial current decay during the first several minutes of the electrolysis, the current remained relatively constant after the addition of approximately 0.5 *F* mol^{-1}. The electrolysis was therefore terminated after the addition of 1.0 and 1.7 *F* mol^{-1} in a series of experiments (see Table I). After the cell contents were allowed to remain under argon for 24 h, the electrolyzed solutions were acidified and product analysis by HPLC was carried out. Significant amounts of unreacted *m*-cyanoanisole remained after electrolysis due to the apparent long lifetime of the radical anion. A major reaction pathway of the radical anion of **2** appears to be catalytic transfer of charge to background in these longtime (>1 h) electrolysis experiments. Product analysis after electrolysis indicated that carbon–carbon bond cleavage with loss of a cyano group to produce anisole could effectively compete with carbon–oxygen bond cleavage (Table I). The relative yield of anisole appeared to increase as the ether concentration decreased. The formation of anisole could be related to the very slow protonation of the radical anion by adventitious water (albeit at low concentration due to alumina treatment of solvent–electrolyte). In addition, dimerization (which is, however, slow) or disproportionation could be responsible for the relatively increased *m*-cyanophenol yields at higher ether concentrations (Table I).

***p*-Cyanoanisole. 1. Cyclic Voltammetry.** *p*-Cyanoanisole (**3**) is reduced to its radical anion at −2.51 V vs. SCE (Figure 4). The cyclic voltammetric wave is chemically irreversible at a scan rate of 0.1 V s^{-1} and a substrate concentration of 2.2 mM. However, upon increasing the scan rate, a reoxidation wave is noted at −2.45 V; at a scan rate of 3 V s^{-1} the ratio of $i_{pa}/i_{pc} = 0.5$ as measured by Nicholson's method.[25] In contrast to the reductive behavior of *o*-cyanoanisole (**1**), the ratio of peak currents (i_{pa}/i_{pc}) is *independent* of concentration over the range 0.26–5.2 mM.[26] Figure 5 illustrates this behavior with a current ratio of 0.5 for more than a decade change in concentration. Thus, the cyclic voltammetric data indicate that the radical anion of **3** reacts by a unimolecular reaction pathway in the above concentration range. Furthermore, no additional oxidation waves are noted, in contrast to the irreversible oxidation wave at −1.1 V noted for **1**.

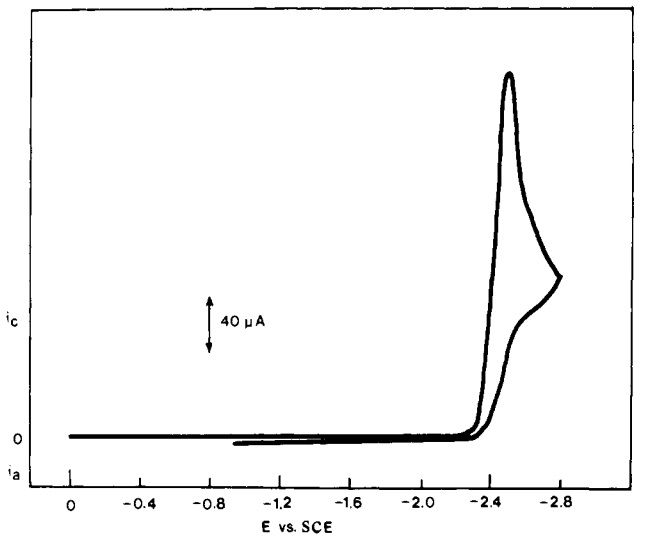

Figure 4. Cyclic voltammogram of 2.2×10^{-3} M *p*-cyanoanisole in 0.2 M TBAP–DMF at a scan rate of 0.1 V s^{-1}. The planar platinum electrode area is ~0.25 cm^2.

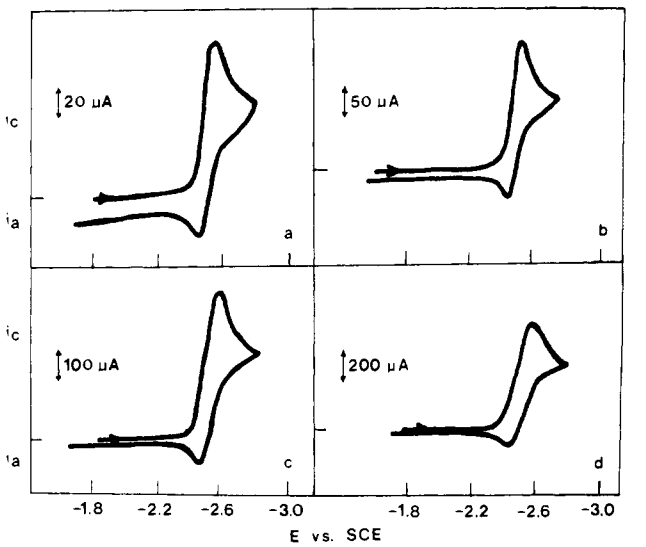

Figure 5. The effect of concentration on the cyclic voltammogram of *p*-cyanoanisole in 0.2 M TBAP–DMF at a scan rate of 3.0 V s^{-1}: (a) 2.5×10^{-4} M; (b) 5.6×10^{-4} M; (c) 1.4×10^{-3} M; (d) 2.2×10^{-3} M.

2. Controlled Potential Electrolysis. The products of electrolysis at −2.6 V were *p*-cyanophenol and methane (Table I), which indicated that carbon–oxygen cleavage was again predominantly occurring via the β (with respect to the cyanophenyl moiety) carbon–oxygen bond. No benzonitrile, 4,4′-dicyanobiphenyl, or higher molecular weight product was observed by HPLC or GLC analysis. With the addition of 2 *F* mol^{-1}, the current efficiency of these electrolyses was less than 100% due to apparent electrocatalytic transfer of charge to electrolyte (i.e., the tetrabutylammonium ion). This type of electrocatalysis is most likely for the meta isomer because of its stability and the para isomer because of its more negative reduction potential. When the concentration of **3** was increased, the current efficiency increased

(25) Nicholson, R. S. *Anal. Chem.* **1966**, *38*, 1406.

(26) This behavior can be compared to the concentration dependent cyclic voltammetric, peak current ratio data for *p*-fluorobenzonitrile.[23,27]

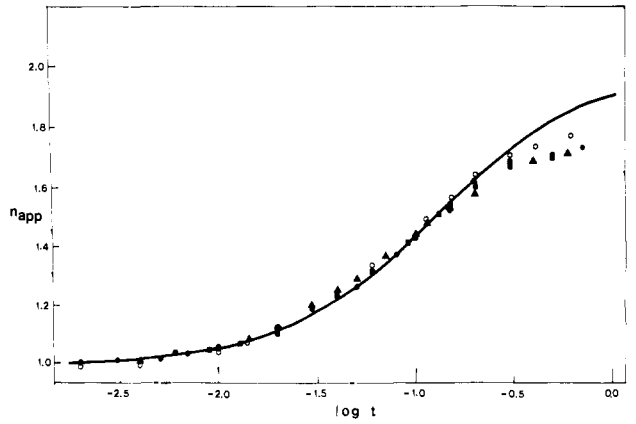

Figure 6. Single potential step chronoamperometric data for the change in electron stoichiometry for the reduction of *p*-cyanoanisole. The solid line was obtained by computer simulation of eq 7–11 with a first-order rate constant (k_1) of 7.0 s^{-1} and $K_{eq} = 10^{30}$.[28] The concentrations of *p*-cyanoanisole in 0.2 M TBAP-DMF are given by the experimental points (■) 2.5×10^{-4} M, (●) 5.6×10^{-4} M, (▲) 1.4×10^{-3} M, and (○) 2.2×10^{-3} M.

and approached 100% for a two-electron process. For example, upon cleavage of 40% of the ether, 0.8 F/mol of charge was injected into the solution (run 7 in Table I). The cyanophenyl moiety of the ether is found as *p*-cyanophenol or unreduced ether in all the experiments. In contrast to *p*-cyanofluorobenzene, no 4,4′-dicyanobiphenyl was detected by chromatographic or electrochemical techniques.[27] The methyl moiety appears exclusively as methane, since no ethane and methyl-substituted aryl compounds, which could result from attack of the methyl radical on unreduced ether, were detected.

3. Kinetics for the Disappearance of the *p*-Cyanoanisole Radical Anion. Cyclic voltammetric data indicated that the radical anion of**3** disappeared by a unimolecular process since the peak current ratios in the cyclic voltammetric experiments were independent of concentration. To further verify this behavior, double potential step chronoamperometric data were obtained as a function of concentration. Since the reduction of **3** remained a diffusion-controlled process at room temperature for times less than 10 ms (vide infra), lower temperatures were employed in order to increase the one-electron diffusion-controlled time domain. When the temperature was lowered to 0 °C, the reduction of **3** remained a diffusion-controlled process (i.e., constant $it^{1/2}/C$) for times up to 30 ms. Double potential step chronoamperometric experiments at concentrations of 0.54 and 2.32 mM were carried out with a forward potential step to −2.70V in order to generate the radical anion. After a time (τ), the cathodic current (i_c) was measured and the potential stepped back to −2.20 V. Anodic currents (i_a) were measured at t_r/τ of 1.2, 1.3, and 1.5. At cathodic electrolysis times of < 20 ms, the current ratio (i_a/i_c) was within experimental error for a chemically reversible system (i.e., at $t_r/\tau = 1.2$, $i_a/i_c = 1.30 \pm 0.02$ compared to the theoretical value of 1.32; at $t_r/\tau = 1.3$, $i_a/i_c = 0.98 \pm 0.05$ vs. 0.948 theoretically; at $t_r/\tau = 1.5$, $i_a/i_c = 0.58 \pm 0.01$ vs 0.598 theoretically). At switching times (τ) greater than 30 ms, the current ratios decreased concomitantly with the increasing $it^{1/2}/C$ values obtained from single potential step chronoamperometric experiments. These data indicated that the electron stoichiometry (or formation of final stable products) was changing concurrently with the disappearance of the radical anion of **3**.

4. Kinetics for the Formation of Products: Single Potential Step Chronoamperometry. Since controlled potential coulometry data indicated that the reduction of *p*-cyanoanisole resulted in β cleavage to *p*-cyanophenol and methane in an overall two-electron process, single potential step chronoamperometry was used to measure the change in electron stoichiometry or product formation as a function of time. The potential was stepped from −2.20 (no electrode reaction) to −2.70 V, at which the concentration of ether should be zero at the electrode surface. The $it^{1/2}/C$ value remained at 37 ± 2 A $s^{1/2}$ mol^{-1} cm^3 at times from 1 to 10 ms. At approximately 10 ms the $it^{1/2}/C$ increased with increasing time; Figure 6 represents a plot of $it^{1/2}/C$ in the form of n_{app} where $n_{app} = (it^{1/2}/C)/(it^{1/2}/C)_{m\text{-tolunitrile}}$. Double potential step chronoamperometry indicated that the disappearance of the radical anion was observable at times greater than 10 ms. Thus, the data again indicate that product formation is concomitant with radical anion disappearance. Furthermore the cyclic voltammetric data support the disappearance of the radical anion by a concentration independent process. The kinetic control of current in the single potential step chronoamperometric experiment was measured as a function of substrate concentration; the $it^{1/2}/C$ value of n_{app} was independent of concentration of ether over a decade change in concentration (0.25–2.2 mM). Thus, the disappearance of the radical anion of **3** and the formation of products occur by a reaction pathway which involves a unimolecular fragmentation of the radical anion as the rate-determining step. A reaction pathway which is consistent with these data and conclusions is an ECEC sequence (eq 7–11) with radical anion cleavage as the

$$ArOCH_3 + e^- \rightleftarrows ArOCH_3^{-}\cdot \quad (7)$$

$$ArOCH_3^{-}\cdot \xrightarrow{k_1} ArO^- + \cdot CH_3 \quad (8)$$

$$\cdot CH_3 + e^- \xrightarrow{\text{electrode}} CH_3^- \quad (9)$$

$$CH_3\cdot + ArOCH_3^{-}\cdot \overset{K_{eq}}{\rightleftharpoons} CH_3^- + ArOCH_3 \quad (10)$$

$$CH_3^- + SH \rightarrow CH_4 + S^- \quad (11)$$

Ar = *p*-cyanophenyl

rate-determining step. This reaction mechanism was computer simulated with the inclusion of the homogeneous electron-transfer nuance (eq 10) with $K_{eq} = 10^{30}$.[28] The selection of a large K_{eq} is based upon the anticipated, more positive $E°$ for the methyl radical than for $ArOCH_3$. The solid line in Figure 6 is the result of the computer simulation with a rate constant (k_1) of 7.0 s^{-1} for the rate-determining radical anion fragmentation reaction. The experimental data fit the theoretical model to an n_{app} value of approximately 1.6. The $it^{1/2}/C$ values remain approximately constant at 60 A $s^{1/2}$ mol^{-1} cm^3 at times greater than 0.4 s, resulting in an $n_{app} = 1.65$. These results suggest that the hydrogen atom abstraction reaction of the methyl radical can compete with further reduction of the methyl radical (eq 12).

$$CH_3\cdot + SH \rightarrow CH_4 + S\cdot \quad (12)$$

Reaction Pathways. These data demonstrate that reductive cleavage of carbon–oxygen bonds can occur in alkyl aryl ethers by reaction pathways which are similar to those observed for carbon–halogen bond cleavages. In the case of the cyano-substituted anisoles, the cyano group plays an important role in determining the reaction pathways of the resultant radical anions. Due to the electron-withdrawing ability of the cyano groups, these radical anions are stable enough to participate in bimolecular reaction pathways. Furthermore, the unpaired electron-density distribution for some of these radical anions is apparently favorable for bond formation in dimerization reactions. The radical anion of *o*-cyanoanisole can be represented by the following resonance structures.[29]

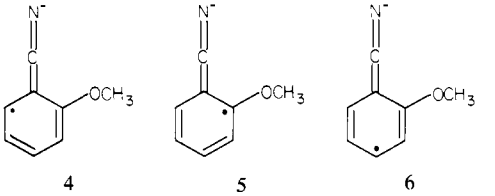

4 5 6

(27) Asirvatham, M. R.; Hawley, M. D. *J. Am. Chem. Soc.* **1975**, *97*, 5024.

(28) Hawley, M. D.; Feldberg, S. W. *J. Phys. Chem.* **1966**, *70*, 3459.

Due to possible steric interactions and Coulombic repulsion considerations, structure **5** will not be favorable toward a dimerization at the site of high unpaired electron density. Although the steric interactions for **4** coupling with **4** or **6** to produce a **4–4** or **4–6** dimer, respectively, are slight, Coulombic repulsion may minimize their formation. Therefore, it is more probable that structure **6** will be the most important contributor toward bond formation with the resultant formation of a **6–6** dimeric dianion of the form 7.[31,32] The proposed dimeric dianion then undergoes

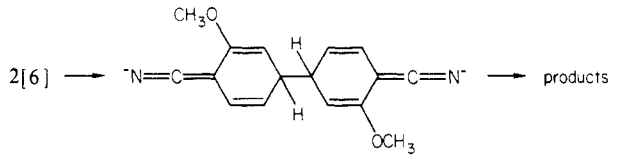

7

a relatively slow intramolecular, electron-transfer reaction with the resultant carbon–oxygen bond cleavage of one of the ether functionalities. The ether cleavage from the dianion occurs β with respect to the aryl group while the other cyanoanisole moiety regains aromaticity by reverting back to the initial substrate.

The radical anion of the para isomer can be represented by three resonance forms, which are similar to the ortho and para positions with respect to the cyano group. None of these forms is apparently conducive to bond formation to produce a dimeric dianion because of the same limitations of steric constraints and Coulombic repulsion, which appear to be important for certain forms (e.g., **5**) of the ortho isomer.

As previously mentioned, the reduction potential of the ortho isomer is approximately 200 mV more positive than that of the para isomer. This is apparently the result of the ortho isomer's ability to accommodate the additional negative charge of the radical anion due to the close proximity of the oxygen-containing methoxy group, which exerts a significant inductive effect. The net result is that the radical anion of the para isomer is inherently less stable than that of the ortho isomer. The inherent instability of the para isomer radical anion and its steric constraints toward dimerization result in a relatively rapid unimolecular fragmentation reaction. This is confirmed by the reaction kinetics demonstrating first-order behavior over a concentration range of 0.2–5 mM.

The meta isomer radical anion is the most stable of the three isomers as expected from electron spin density calculations.[34] These calculations indicate a significant decrease in relative electron density in the meta position, relative to a strong electron-withdrawing group. The result is that the *m*-cyanoanisole is stable toward heterolytic bond cleavage at the meta carbon center.[35-37] Alternative reaction pathways including slow protonation followed by carbon–carbon bond cleavage at the cyano-substituted carbon to produce anisole then become more important.

In summary, carbon–oxygen bond cleavage pathways in the cyanoanisoles are quite different for each isomer due to structural and therefore stability differences for the radical anion intermediates. However, the reaction pathways are analogous to those observed in other radical anion reactions including carbon–halogen bond cleavage reactions. The cyano group, when substituted on aryl systems, appears to play an important role in the reaction pathways, which may include carbon–heteroatom bond cleavage, of these types of radical anions.

Experimental Section

Instrumentation. Cyclic voltammetric, chronoamperometric, and controlled potential electrolysis experiments were carried out with a PAR Model 173 potentiostat equipped with a Model 179 digital coulometer. Cyclic voltammetric waveforms were generated by using a digital-controlled, multifunction generator[38] coupled with the PAR 173. Cyclic voltammetric data for scan rates less than 200 mV/s were recorded on a Soltec X-Y recorder. Cyclic voltammeric data for scan rates greater than 200 mV/s were recorded with a Tektronix 5103N storage oscilloscope which was equipped with a Type 5A20N differential amplifier and a Model C-5 Polaroid camera. Potential control and data acquisition for single and double potential step chronoamperometric studies were performed with an Apple II (64K) microcomputer, which was interfaced with the PAR 173 potentiostat and the PAR 179 current-to-voltage converter output. The microcomputer was equipped with a California Computer Systems Model 7424 clock board for timing control and an Interactive Structures analogue-to-digital (A/D) A113 converter board. The A/D (12 bit) has a conversion time of 20 μs and the board is equipped with a software programmable analogue preamplifier for signal conditioning. Data acquisition at the 1-ms time level was achieved with this instrumental arrangement by use of assembly-level language for the data-sampling subroutine. Control of the PAR 173 was achieved by the digital-to-analogue outputs of the game-paddle socket of the Apple II microcomputer. All electrochemical measurements were made with positive feedback electronic compensation for ohmic potential loss.

Chemicals. The three isomers of cyanoanisole [ortho (Pfaltz and Bauer), meta (Aldrich), and para (Aldrich)] were checked for purity by both gas and high-pressure liquid chromatographic techniques. Electrochemical grade tetra-*n*-butylammonium perchlorate (TBAP) (Southwestern Analytical Chemicals) was dried under vacuum at 100 °C for 24 h and used as the supporting electrolyte. Spectroscopic grade dimethylformamide (DMF) (Burdick and Jackson) was employed as the electrochemical solvent. The DMF with dissolved 0.2 M TBAP was dried with freshly activated, anhydrous alumina.[39] Woelm W200 neutral alumina grade Super I was activated by heating under vacuum at 550 °C for 24 h. The alumina which was retained under a vacuum was then transferred to a Vacuum Atmospheres HE-43-2 Dri-Lab glovebox equipped with a HE-493 Dri-Train. The DMF solution of electrolyte was dried by passage through a column of activated alumina in the glovebox. The DMF–TBAP solution was then transferred to an all-glass vacuum line and oxygen was removed by several freeze–pump–thaw cycles. Dry, deoxygenated DMF–TBAP solutions were then stored in the glovebox prior to use. All subsequent solutions for electrochemical measurements were prepared in the glovebox, whose atmosphere was periodically checked for oxygen and water content with an exposed 25-W tungsten filament light bulb (typical lifetimes of >3 days indicated sub-ppm levels of contaminants in the argon atmosphere).

Electrodes and Cells. Solvent and electroactive chemicals were introduced into airtight, all-glass electrochemical cells in the glovebox. The electrochemical cells for cyclic voltammetry, chronoamperometry, and controlled potential electrolysis have been previously described.[37]

The working electrode for cyclic voltammetric and chronoamperometric experiments was modified Beckman platinum button electrode (no. 39273) with a geometric area of approximately 0.25 cm^2. Longtime chronoamperometric studies ($t > 5$ s) were performed on a platinum electrode (geometric area ca. 0.95 cm^2) which was modified by the addition of a 6-mm glass mantle to minimize the effect of edge diffusion.[40] Control experiments on this latter electrode using nitrotoluene as the electroactive species indicated that chronoamperometric $it^{1/2}$ values were diffusion controlled for $t \leq 800$ s.

Product Analysis. Analysis of products obtained in controlled potential electrolyses was accomplished by high-pressure liquid chromatography on a Waters Associates 6000A HPLC equipped with a Model 660 solvent programmer. The electrolyzed solutions were acidified with $HClO_4$ and directly injected onto a 0.25 in. × 25 cm Alltech C18 column with a 10-μm mean particle size packing. Mobile-phase composition (acetonitrile/4% acetic acid in water) was varied by use of the solvent pro-

(29) These structures are based on the model that the only important valence bond structures are those in which the negative charge is localized on the strong electron-withdrawing substituent.[30]

(30) Schug, J. C.; Brown, T. H.; Karplus, M. *J. Chem. Phys.* **1962**, *37*, 330.

(31) Ab initio molecular orbital calculations have shown that the kinetically preferred sites of protonations for substituted benzene radical anions are ipso and para for π-acceptor substituents such as the cyano group.[33]

(32) A referee kindly noted that coupling reactions which lead to the formation of *p*-quinonoid-type structures are generally favored over *o*-quinonoid structures.

(33) Birch, A. J.; Hinde, A. L.; Radom, L. *J. Am. Chem. Soc.* **1980**, *102*, 3370.

(34) Rieger, P. H.; Fraenkel, G. K. *J. Chem. Phys.* **1962**, *37*, 2795.

(35) Alwair, K.; Grimshaw, J. *J. Chem. Soc. Perkin Trans 2* **1973**, 1811.

(36) Grimshaw, J.; Trocha-Grimshaw, J. *J. Electroanal. Chem.* **1974**, *56*, 443.

(37) Gores, G. J.; Koeppe, C. E.; Bartak, D. E.; *J. Org. Chem.* **1979**, *44*, 380.

(38) Bartak, D. E.; Hundley, H. K.; Van Swaay, M.; Hawley, M. D. *Chem. Instrum. (N.Y.)* **1972**, *4*, 1.

(39) Jensen, B. S.; Parker, V. D. *J. Am. Chem. Soc.* **1975**, *97*, 5211.

(40) We thank Professor M. D. Hawley, Kansas State University, for a gift of this electrode.

grammer. Products were identified by spiking techniques. Calibration curves were prepared daily and employed for product quantitation. Analysis for methane gas was accomplished by gas chromatography with molecular sieve Type 5A columns.[41] Gas chromatographic analysis of other products was carried out on a Varian Aerograph Series 2100 gas chromatograph equipped with $^1/_8$-in., all-glass OV-17 columns and FID detectors.

(41) Gas analyses by gas chromatography were generously performed by the UND Engineering Experiment Station.

Acknowledgment. Grateful acknowledgement is made to the U.S. Department of Energy for supporting this research through Grant No. DE-FG22-80PC30227. Financial support to M.D.K. was made possible by a North Dakota MMRRI Fellowship. The encouragement and initial support by Professor M. D. Hawley are gratefully acknowledged. We thank Dr. Virgil Stenberg for helpful discussions.

Registry No. 1, 6609-56-9; **1** radical anion, 89596-85-0; **2**, 1527-89-5; **2** radical anion, 68271-94-3; **3**, 874-90-8; **3** radical anion, 68271-93-2.

Tri-*s*-triazine: Synthesis, Chemical Behavior, and Spectroscopic and Theoretical Probes of Valence Orbital Structure

Manouchehr Shahbaz,[†] Shigeyuki Urano,[†] Pierre R. LeBreton,*[†] Mitchell A. Rossman,[‡] Ramachandra S. Hosmane,[‡] and Nelson J. Leonard*[‡]

Contribution from the Department of Chemistry, University of Illinois at Chicago, Chicago, Illinois 60680, and the Department of Chemistry, University of Illinois at Urbana-Champaign, Urbana, Illinois 61801. *Received May 26, 1983*

Abstract: The synthesis, physical properties, and chemical properties of unsubstituted tri-*s*-triazine (1,3,4,6,7,9,9b-heptaazaphenalene) are reported. The abbreviated synthesis consisted of a two-step procedure whereby 2,4-diamino-1,3,5-triazine was treated with methyl *N*-cyanomethanimidate and NaOMe in Me_2SO/MeOH to give 2,4-bis(*N'*-cyano-*N*-formamidino)-1,3,5-triazine, which was subjected to short vacuum pyrolysis to give tri-*s*-triazine. The compound gave no evidence of (a) formation of π complexes with either electron-donor or electron-acceptor organic partners, (b) protonation, (c) alkylation, or (d) N-oxidation, yet it formed complexes with silver salts and decomposed in water. Photoelectron spectroscopic studies of tri-*s*-triazine have provided ionization potentials associated with the six highest occupied π and six highest occupied lone-pair orbitals. Interpretation of the photoelectron spectrum has been aided by results from semiempirical HAM/3 and from ab initio, GAUSSIAN70, quantum mechanical calculations. The detailed picture of valence orbital structure provides insight concerning the low basicity and the overall high chemical stability of tri-*s*-triazine.

Tri-*s*-triazine (**1**)[1,2] is the ultimate member of the alternating C,N azacycl[3.3.3]azine series. The first member of the series is called cycl[3.3.3]azine (**2**)[3,4] and contains three fused conjugated

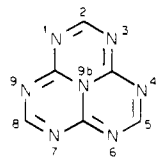

1

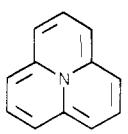

2

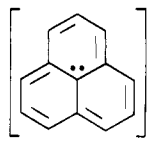

3

six-membered rings held planar by three covalent bonds to an internal nitrogen atom.[5,6] Cycl[3.3.3]azine is formally isoelectronic with the phenalenide anion (**3**) containing an all-carbon skeleton[7,8] and, with the aza compounds in the series, has been the subject of numerous theoretical calculations and predictions.[9-16] The considerable theoretical interest in the cycl[3.3.3]azine series is derived from the 12-π-electron periphery and the question of the involvement of the n electrons of the central N. Moreover, although members of the series containing from 0 to 6 N atoms in the periphery are formally isoelectronic, they exhibit widely different electronic and chemical properties.[10] For example, cycl[3.3.3]azine (**2**) is chemically reactive and readily undergoes oxidation and addition reactions,[3,4] while 1,3,4,6,7,9-hexaazacycl[3.3.3]azine or tri-*s*-triazine (**1**)[2] is chemically unreactive except for its facile decomposition by water.

Scheme I

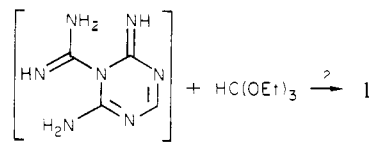

4

Scheme II

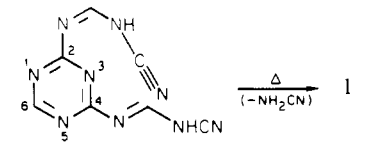

5

The properties of heat stability, low solubility, and little chemical reactivity are characteristic of a group of related nitrogen com-

[†] Department of Chemistry, University of Illinois at Chicago.
[‡] Department of Chemistry, University of Illinois at Urbana-Champaign.

(1) Other names of **1** include cyamelurine, 1,3,4,6,7,9,9b-heptaazaphenalene, *s*-heptazine, and 1,3,4,6,7,9-hexaazacycl[3.3.3]azine.
(2) Hosmane, R. S.; Rossman, M. A.; Leonard, N. J. *J. Am. Chem. Soc.* **1982**, *104*, 5497.
(3) Farquhar, D.; Leaver, D. *Chem. Commun.* **1969**, 24.
(4) Farquhar, D.; Gough, T. T.; Leaver, D. *J. Chem. Soc., Perkin Trans. 1* **1976**, 341.
(5) Windgassen, R. J., Jr.; Saunders, W. H., Jr.; Boekelheide, V. *J. Am. Chem. Soc.* **1959**, *81*, 1459.

0002-7863/84/1506-2805$01.50/0